Liquid-Phase Hydrogenation Kinetics of Isooctenes on Ni/Al_2O_3

M. S. Lylykangas, P. A. Rautanen, and A. O. I. Krause
Helsinki University of Technology, Department of Chemical Technology, FIN-02015 HUT, Finland

The kinetics of the hydrogenation of isooctenes [2,4,4-trimethyl-1-pentene (TMP-1), and 2,4,4-trimethyl-2-pentene (TMP-2)] to isooctane (2,2,4-trimethylpentane) was studied on a commercial Ni/Al_2O_3 catalyst in a three-phase reactor. Experiments showed that nickel is a highly active catalyst for the reactions. In addition to the hydrogenation reactions, slow isomerization occurred between TMP-1 and TMP-2. Kinetic equations were derived based on the Horiuti–Polanyi mechanism, involving a half-hydrogenated surface intermediate and rate limitation in the first hydrogen addition. Isomerization was assumed to take place via the partly hydrogenated intermediate, since no isomerization products were observed in the absence of hydrogen. The dynamic reactor model consisted of material balances for the gas and liquid phases, as well as for the porous catalyst particles. The estimated activation energies for the hydrogenation of TMP-1 and TMP-2 were 34 and 49 kJ/mol, respectively. The model described the experimentally recorded data accurately.

Introduction

Methyl *tert*-butylether [2-methoxy-2-methyl propane (MTBE)] is a widely used component in gasoline because of its high octane rating and low emissions of carbon monoxide and hydrocarbons. Unfortunately, claims that it is contaminating ground water are threatening the future of MTBE as a fuel component. The demand for MTBE is expected to decrease considerably in the near future because of the forthcoming regulations on the maximum oxygen content of gasoline (Trotta et al., 1999). Refineries are, thus, being forced to search for new gasoline components with a high octane number and at the same time decide about the future of their existing MTBE plants and feedstocks.

One possible solution to the problem is a new process technology that allows refineries to convert their MTBE plants to the production of isooctane [2,2,4-trimethylpentane (IO)]. Isooctane is the reference compound for the measurement of octane and, by definition, both MON and RON are 100, which is higher than the ratings of the normal commercially produced alkylates. It could thus be used as a replacement for both the volume and the octane of MTBE in gasoline. Two companies have introduced process configurations for isooctane units (Sloan et al., 2000; Trotta et al., 1999). The main principle is the same in both: isobutene is first selectively dimerized to isooctenes: 2,4,4-trimethyl-1-pentene (TMP-1), and 2,4,4-trimethyl-2-pentene (TMP-2), and in a second stage the isooctenes are hydrogenated to isooctane. The present MTBE reactor can be used in the dimerization mode. Temperature, pressure, and, isobutene, conversion are almost the same as in the MTBE synthesis, and the normal MTBE catalyst can be applied (Sanfilippo, 2000). Thus, the existing MTBE processes can be replaced by the production of isooctane without fundamental changes in the unit.

The present work focuses on the hydrogenation stage of the isooctane process. The kinetics of the hydrogenation of TMP-1 and TMP-2 on a commercial Ni/Al_2O_3 catalyst was studied in a three-phase reactor. A kinetic model was developed on the basis of the Horiuti–Polanyi mechanism, and the model parameters were estimated from the experimental data. In an earlier study on the equilibrium composition of the isooctene mixture (Karinen et al., 2000), we found that the molar ratio of TMP-1 and TMP-2 is about 4:1 in the temperature range from 50°C to 100°C, and it shifts slightly toward TMP-2 as a function of temperature. If the thermodynamic equilibrium between TMP-1 and TMP-2 is known and mixtures deviating from the equilibrium composition are used

Correspondence concerning this article should be addressed to M. S. Lylykangas.

as reactants, information can be obtained on the hydrogenation reactivities of the two isomers and on the rate of their isomerization. This information can then be utilized in the process development of an isooctane unit.

Experimental Studies

A commercial nickel-alumina catalyst (16.6 wt. % Ni, 108 m^2/g specific surface area, 0.37 cm^3/g mean pore volume) was used in all the experiments. Internal mass- and heat-transfer limitations were minimized by crushing the catalyst to 0.5–0.6-mm particle size. Before each experiment, the catalyst was dried at 110°C in nitrogen and then reduced *in situ* at 400°C for 2 h in hydrogen flow. About 35 mg of fresh catalyst was loaded in the reactor before each experiment, and the pretreatment procedure was automated to achieve reproducible activity.

The equilibrium mixture of TMP-1 and TMP-2 (ratio 4:1, ~95%) was supplied by Fluka and cyclohexane, which was used as the solvent, was from AnalaR (99.5%). Feeds rich in TMP-1 or TMP-2 were obtained by separating the other isomer from the equilibrium mixture by distillation (the boiling points of TMP-1 and TMP-2 are 101.5°C and 105.0°C, respectively). Liquid-phase reactant solutions were flushed with nitrogen before the experiments in order to remove any traces of dissolved oxygen. Both hydrogen (99.999%) and nitrogen (99.9999%) were supplied by AGA and were used as received.

Hydrogenation experiments were carried out in a three-phase Robinson–Mahoney reactor (50 mL), which was operated in CSTR mode. The reactor was equipped with a fixed catalyst basket and a magnetic stirrer. The gas and liquid flows in the feed were regulated by mass flow controllers. Reaction pressure was maintained at the desired level (±0.1 bar) by regulating the gas outlet stream, and temperature was adjusted with a programmable temperature controller (±0.5°C). The product samples were taken through an automatic on-line valve and analyzed by a gas chromatograph with a fused-silica capillary column and an FI detector. A simplified picture of the setup is presented in Figure 1.

Reaction temperature, pressure, and initial concentrations were varied during the experiments: temperatures from 35°C to 95°C with 20°C intervals, and pressures from 10 to 40 bar with 10-bar intervals. The total concentration of isooctenes was 5 or 15 mol % with varying ratios of the isomers. A typical run was divided into periods of 5 to 12 h, each with a different combination of the reaction parameters. A standard period with reference conditions (5 mol % equilibrium solution, 75°C, 20 bar) was included at the beginning and end of each run to monitor the catalyst activity. Experiments were started with liquid and nitrogen flows until the reactor dynamics reached steady state. Thereafter, the reaction was initiated by changing the gas feed to hydrogen, and a precise starting time for the reaction was specified.

Qualitative Observations

The kinetic experiments showed that nickel is a highly active catalyst for the hydrogenation of isooctenes. With a WHSV of about 1,400 h^{-1}, the conversions of TMP-1 and TMP-2 varied from about 20% to 45% and 5% to 30%, respectively. Besides isooctane, no other saturated products were formed, but some isomerization between TMP-1 and TMP-2 was observed. TMP-1 was the more reactive alkene toward hydrogenation, but the hydrogenation rates of both isomers exceeded the double-bond isomerization rate, as the

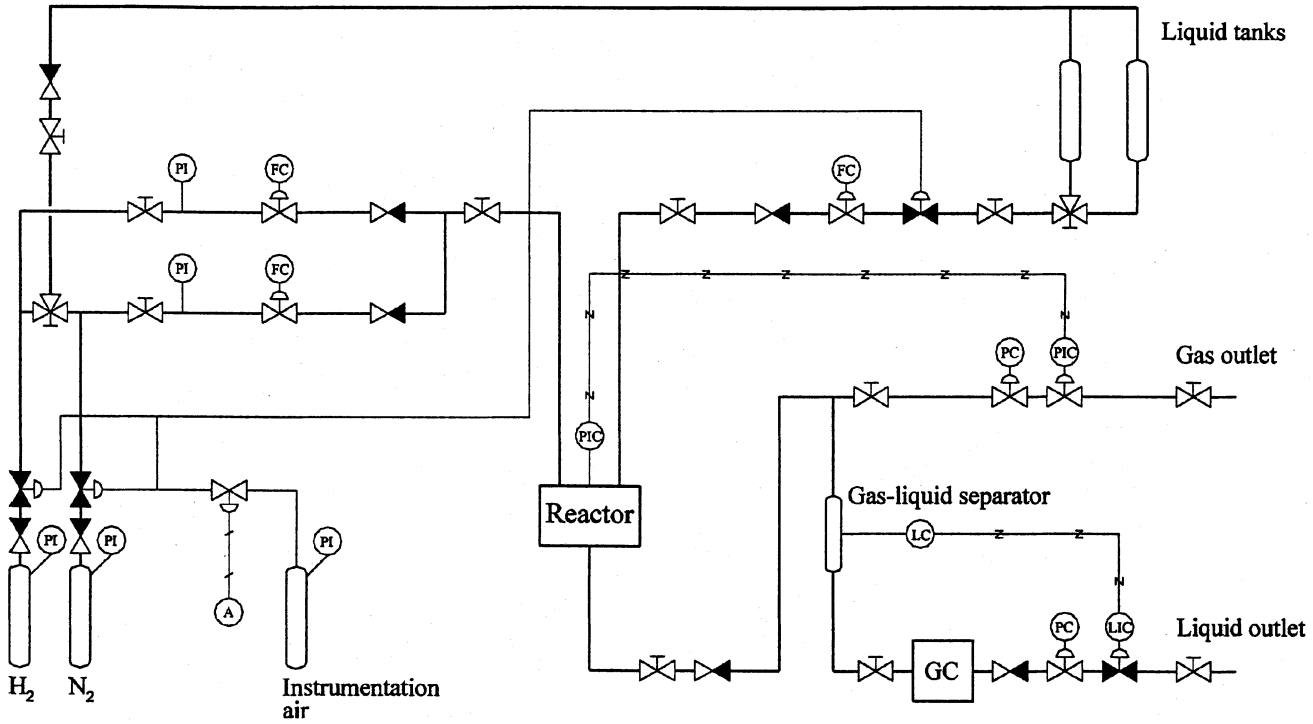

Figure 1. Experimental setup for the hydrogenation of TMP – 1 and TMP – 2.

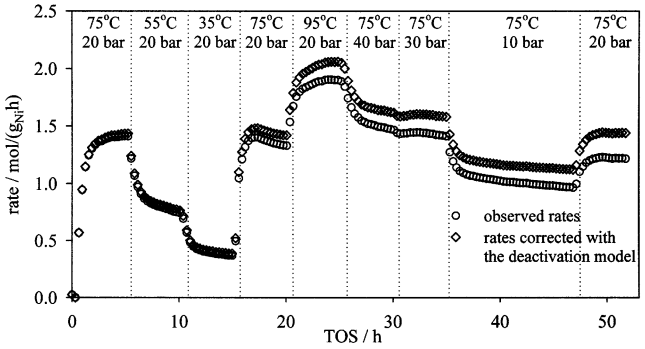

Figure 2. Rates of the formation of isooctane in experiment A, where the feed was 5 mol % equilibrium mixture of TMP − 1 and TMP − 2 in cyclohexane.

Temperature and pressure in each stage are shown at the top of the figure.

amount of saturated product (IO) always exceeded the amount of isomerization product (TMP-1 or TMP-2). For example, when pure TMP-1 was used as the reagent, the formation rate of isooctane was typically 5–10 times higher than the formation rate of TMP-2. The hydrogenation rates increased faster than the isomerization rate with temperature and pressure, and, therefore, the relative importance of the double-bond isomerization decreased with increasing alkene conversion. Because of TMP-1's higher reactivity compared with TMP-2 and slow isomerization rate, the ratio TMP-1/TMP-2 shifted slightly toward TMP-2 when an equilibrium mixture was used as the reagent.

The hydrogenation rates increased exponentially as a function of temperature according to the Arrhenius equation, and the apparent activation energy for the product formation was 26 kJ/mol. The effect of pressure on the reaction rates was less pronounced, especially at hydrogen pressures above 30 bar. Figure 2 depicts the rate of the product formation at different temperatures and pressures as a function of time on stream in an experiment where the feed was 5 mol % equilibrium mixture of TMP-1 and TMP-2.

Some catalyst deactivation was observed during the experiments. In Figure 2, this effect is seen as a slight decrease in the reaction rate in the last relative to the first stage of the run (performed under similar conditions). Deactivation was assumed to be due to the formation of hydrogen-deficient species, since the original activity was recovered by flushing the used catalyst with hydrogen at an elevated temperature. However, no analytical tools were available for the quantitative description of these compounds, and the deactivation was eliminated from the results by an empirical first-order deactivation model. The deactivation parameter was fitted separately in each run on the basis of rates recorded during the standard periods. Figure 2 depicts, in addition to the experimental rates, calculated rates corresponding to the initial activity.

Reproducibility of the experimental data was examined by comparing the formation rates of isooctane in the first standard period of each experiment (75°C, 20 bar, 5 mol % of equilibrium mixture of isooctene in cyclohexane). These replicates showed that the variation in the rates was about $\pm 10\%$ from the average. This variation was assumed to be due to inhomogeneities in the catalyst, and it was eliminated in the kinetic modeling by normalizing the experiments, that is, multiplying the catalyst mass of each experiment by a correction factor so that the rates in the standard periods of the experiments were equal.

Model for the Hydrogenation Kinetics

The hydrogenation of alkene double bonds on metal catalysts is typically described by the Horiuti–Polanyi mechanism (Horiuti and Polanyi, 1934), which was originally developed for the hydrogenation of ethene, but has more recently been applied to alkenes of varying chain lengths (McLeod and Gladden, 1999; Cortright et al., 1998). According to the classic Horiuti–Polanyi mechanism, the alkene is chemisorbed on the catalyst surface, accompanied by the opening of the double bond and a two-step addition of dissociatively adsorbed hydrogen. There is evidence, however, that this mechanism is not the only one involved in the hydrogenation of alkenes on nickel and noble metal catalysts: the alkene may also adsorb in π-configuration (Mintsa-Eya et al., 1983; Kiperman, 1986). Fukushima and Ozaki (1979) have reported experimental evidence to show that the π-complex between Ni and alkene is the main hydrogenation intermediate. Recent theoretical calculations support this observation. Neurock and van Santen (2000) studied the structure of ethene adsorbed on a well-defined palladium surface using first-principle density functional quantum chemical calculations. Their results showed that, at low surface coverage of ethene, hydrogenation occurs via a di-σ-intermediate, whereas at higher coverage the π-bound state predominates. Concentrations are substantially higher in the liquid phase than in the gas phase, and we assume, therefore, a surface structure π-coordinated to a single active site.

The described mechanism is applied for the reactions of TMP-1 and TMP-2 in Table 1. Desorption of isooctane on nickel is regarded as irreversible because the adsorption of saturated hydrocarbons is weaker than the adsorption of the corresponding alkenes, and dehydrogenation would occur only at considerably higher temperatures (Kiperman, 1986).

Table 1. Reaction Steps in the Hydrogenation of TMP-1 and TMP-2 According to the Proposed Mechanism

Step	Reaction Equation	Rate
a	$\text{TMP-1} + * \underset{k_{-1}}{\overset{k_1}{\rightleftharpoons}} \text{TMP-1}*$	$k_1 c_{\text{TMP-1}} \Theta_v - k_{-1} \Theta_{\text{TMP}-1}$
b	$\text{TMP-2} + * \underset{k_{-2}}{\overset{k_2}{\rightleftharpoons}} \text{TMP-2}*$	$k_2 c_{\text{TMP-2}} \Theta_v - k_{-2} \Theta_{\text{TMP}-2}$
c	$\text{H}_2 + 2* \underset{k_{-H}}{\overset{k_H}{\rightleftharpoons}} 2\text{H}*$	$k_{\text{H}} c_{\text{H}_2} \Theta_v^2 - k_{-\text{H}} \Theta_H^2$
d	$\text{TMP-1}* + \text{H}* \underset{k_{-3}}{\overset{k_3}{\rightleftharpoons}} Y* + *$	$k_3 \Theta_{\text{TMP-1}} \Theta_{\text{H}} - k_{-3} \Theta_Y \Theta_v$
e	$\text{TMP-2}* + \text{H}* \underset{k_{-4}}{\overset{k_4}{\rightleftharpoons}} Y* + *$	$k_4 \Theta_{\text{TMP-2}} \Theta_{\text{H}} - k_{-4} \Theta_Y \Theta_v$
f	$Y* + \text{H}* \underset{k_{-5}}{\overset{k_5}{\rightleftharpoons}} \text{IO}* + *$	$k_5 \Theta_Y \Theta_{\text{H}} - k_{-5} \Theta_{\text{IO}} \Theta_v$
g	$\text{IO}* \xrightarrow[\text{Rapid}]{k_6} \text{IO} + *$	$k_6 \Theta_{\text{IO}}$

Isomerization between TMP-1 and TMP-2 was assumed to take place via the common half-hydrogenated intermediate, *Y*. Experimental evidence for this was obtained by performing experiments at the same temperatures and pressures with pure TMP-1 and TMP-2, but in the absence of hydrogen (in nitrogen flow). In this case, no traces of isomerization products were observed. In addition, a slow isomerization rate compared with the hydrogenation rates in the kinetic experiments implied rate limitation in the first hydrogen insertion in the double bonds of adsorbed TMP-1 and TMP-2. Jonker et al. (1997) also reported that this step is probably rate-determining in the hydrogenation of C=C double bond on a nickel catalyst.

In the derivation of the kinetic equations, it was assumed that the adsorption of the reactants is fast enough for the quasi-equilibrium hypothesis to be applied

$$K_1 = \frac{\Theta_{\text{TMP-1}}}{c_{\text{TMP-1}}\Theta_v} \tag{1}$$

$$K_2 = \frac{\Theta_{\text{TMP-2}}}{c_{\text{TMP-2}}\Theta_v} \tag{2}$$

$$K_{\text{H}} = \frac{\Theta_{\text{H}}^2}{c_{\text{H}_2}\Theta_v^2} \tag{3}$$

Furthermore, the pseudo-steady-state hypothesis was applied for the half-hydrogenated intermediate *Y*

$$r_{Y^*} = k_3\Theta_{\text{TMP-1}}\Theta_{\text{H}} - k_{-3}\Theta_Y\Theta_v + k_4\Theta_{\text{TMP-2}}\Theta_{\text{H}} - k_{-4}\Theta_Y\Theta_v - k_5\Theta_Y\Theta_{\text{H}} = 0 \tag{4}$$

When Eqs. 1–4 are solved with respect to the fractional surface coverages, and these expressions are substituted in the site balance

$$\Theta_v = 1 - \Theta_{\text{TMP-1}} - \Theta_{\text{TMP-2}} - \Theta_{\text{H}} - \Theta_Y \tag{5}$$

the surface coverages can be expressed as a function of the bulk concentrations ($\Theta_{IO} = 0$ due to the rapid and irreversible desorption of isooctane), and the rate equations for TMP-1 and TMP-2 can be written as

$$-r_{\text{TMP-1}} = k_3\Theta_{\text{TMP-1}}\Theta_{\text{H}} - k_{-3}\Theta_Y\Theta_v = \frac{k_3K_1\sqrt{K_{\text{H}}}\,c_{\text{TMP-1}}\sqrt{c_{\text{H}_2}} - k_{-3}\alpha}{\left(1 + K_1c_{\text{TMP-1}} + K_2c_{\text{TMP-2}} + \sqrt{K_{\text{H}}c_{\text{H}_2}} + \alpha\right)^2} \tag{6}$$

and

$$-r_{\text{TMP-2}} = k_4\Theta_{\text{TMP-2}}\Theta_{\text{H}} - k_{-4}\Theta_Y\Theta_v = \frac{k_4K_2\sqrt{K_{\text{H}}}\,c_{\text{TMP-2}}\sqrt{c_{\text{H}_2}} - k_{-4}\alpha}{\left(1 + K_1c_{\text{TMP-1}} + K_2c_{\text{TMP-2}} + \sqrt{K_{\text{H}}c_{\text{H}_2}} + \alpha\right)^2} \tag{7}$$

where

$$\alpha = \frac{(k_3K_1c_{\text{TMP-1}} + k_4K_2c_{\text{TMP-2}})\sqrt{K_{\text{H}}c_{\text{H}_2}}}{k_{-3} + k_{-4} + k_5\sqrt{K_{\text{H}}c_{\text{H}_2}}} \tag{8}$$

The first terms in the numerator of the rate equations describe the forward reactions of the alkenes (hydrogenation), and the second terms correspond to the backward reactions and isomerization.

The results showed that the formation rate of the hydrogenation product (isooctane) was 5–10 times higher than the formation rate of the isomerization product (TMP-1 or TMP-2), even when pure isomers were used in the feed. This implies that the isomerization did not have a significant effect on the hydrogenation reactions under the studied conditions. The role of the isomerization is shown in Figure 3, where the ratio of TMP-1 and TMP-2 in the feed and in the reactor outlet is plotted in two experimental runs. Reference conditions and the equilibrium mixture were applied in the first and last stages, and mixtures rich in TMP-2 (left) and TMP-1 (right) were used in other stages. Figure 3 confirms that the isomerization is much slower than the hydrogenation reactions: in both runs the ratio of TMP-1/TMP-2 in the outlet

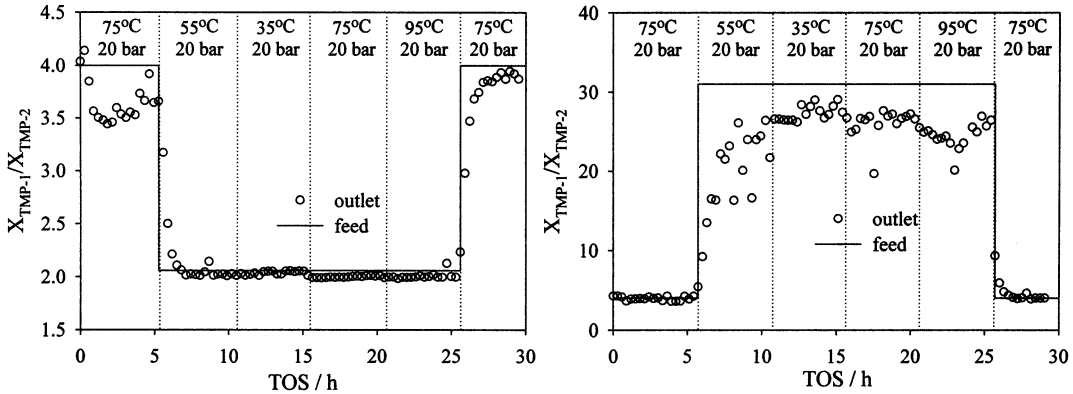

Figure 3. The molar fractions of TMP − 1 and TMP − 2 as a function of time on stream (TOS) in two experimental runs with different feed compositions.

Total molar fraction of isooctenes was 5 mol %.

stays close to the value in the feed. If isomerization were fast, the ratio would reach the equilibrium value in all stages. In view of slow isomerization, the rate equations (Eqs. 6 and 7) were simplified by assuming the isomerization terms in the numerator to be zero. In addition, the coverage of the half-hydrogenated intermediate was assumed to be negligible relative to the coverages of the bulk reactants (α set to 0 in the denominator). The following rate equations were obtained after replacing the parameter groups by lumped parameters $k_{\text{TMP-1}}$, $k_{\text{TMP-2}}$, $K_{\text{TMP-1}}$, and $K_{\text{TMP-2}}$:

$$-r_{\text{TMP-1}} = \frac{k_{\text{TMP-1}} c_{\text{TMP-1}} \sqrt{c_{\text{H}_2}}}{\left(1 + K_{\text{TMP-1}} c_{\text{TMP-1}} + K_{\text{TMP-2}} c_{\text{TMP-2}} + \sqrt{K_{\text{H}} c_{\text{H}_2}}\right)^2} \tag{9}$$

and

$$-r_{\text{TMP-2}} = \frac{k_{\text{TMP-2}} c_{\text{TMP-2}} \sqrt{c_{\text{H}_2}}}{\left(1 + K_{\text{TMP-1}} c_{\text{TMP-1}} + K_{\text{TMP-2}} c_{\text{TMP-2}} + \sqrt{K_{\text{H}} c_{\text{H}_2}}\right)^2} \tag{10}$$

where the temperature dependency of the rate constants $k_{\text{TMP-1}}$ and $k_{\text{TMP-2}}$ was described by the Arrhenius equation. Adsorption equilibrium constants K_i were assumed independent of temperature. Usually, the temperature dependency of K_i is described with the van't Hoff law. However, the heat of adsorption is known to decrease as the surface coverage increases, as originally reported by Temkin (1979), and the temperature dependency of K_i was therefore assumed small in this study, because the surface coverage is typically large in the liquid phase.

Our finding that isomerization was insignificant in the hydrogenation of isooctenes is in contrast to the results of Peque and Maurel (1969), who studied the hydrogenation of TMP-1 and TMP-2 on Raney nickel at 25°C and under 1.0-bar hydrogen pressure. Under those reaction conditions, isomerization played an important role in the reaction when reactants were the pure isomers. The most likely explanation for this dissimilarity is the different conditions under which the experiments were performed. Since the hydrogenation rates increased faster than the isomerization rate with hydrogen pressure, one would expect the role of isomerization to be less pronounced at elevated pressures (this work) than at ambient pressure (Peque and Maurel, 1969).

Reactor Model

The dynamic reactor model consisted of the material balances in the gas and liquid phases for all compounds present in the reaction mixtures

$$\frac{dn_i^G}{dt} = F_{\text{in},i}^G - V_R \cdot N_{GL,i} a_{GL} - F_{\text{out},i}^G \tag{11}$$

and

$$\frac{dn_i^L}{dt} = F_{\text{in},i}^L + V_R \cdot N_{GL,i} a_{GL} + V_R \cdot N_{LS,i} a_{LS} - F_{\text{out},i}^L \tag{12}$$

where V_R is the volume of the reactor (50 mL) and $N_{LS,i} a_{LS}$ is the mass-transfer rate of component i at the liquid–solid interface (observed reaction rate). The molar fluxes between the gas and liquid phases $N_{GL,i} a_{GL}$ were calculated by the two-film theory. Preliminary experiments showed that the gas–liquid mass transfer had no effect on the overall rates. Therefore, high values were given for the mass-transfer coefficients in the gas and liquid films: $\kappa_G a_{GL} = 1.0 \times 10^4\ \text{s}^{-1}$ and $\kappa_L a_{GL} = 1.0 \times 10^2\ \text{s}^{-1}$. The outlet molar fluxes of gas and liquid phases were evaluated by simulating a P-controller

$$F_{\text{out}} = K_p \left(V_{\text{calc}} - V_{\text{exp}}\right)^2 \tag{13}$$

The experimental volumes were estimated from a step-response experiment ($V_{\text{exp}}^L = 30.7$ mL, $V_{\text{exp}}^G = 19.3$ mL), and the constant K_p was given a value of 10^9 mol/(m^{6}s). Calculated volumes of the gas and liquid phases were obtained as a sum of the partial molar volumes of the components. These were estimated with the Peng–Robinson (PR) equation of state, which Park et al. (1995) and Moysan et al. (1983) have shown to be an accurate method for estimating mixtures of hydrogen and alkane/alkene. Estimations with the PR equation of state showed that the molar fraction of organic compounds in the gas phase and hydrogen in the liquid phase varied between 1.2 and 9.1 mol %, and 0.8 and 3.3 mol %, respectively.

The mass-transfer limitation inside the catalyst particles could not be eliminated in the experiments, and mole balances for each component were written assuming spherical geometry

$$\frac{\partial c_i}{\partial t} = \frac{D_{\text{eff},i}}{\epsilon_p r_p^2} \left(\frac{\partial^2 c_i}{\partial \lambda^2} + \frac{2}{\lambda} \frac{\partial c_i}{\partial \lambda} \right) + r_i \cdot \frac{\rho_p}{\epsilon_p} \tag{14}$$

with the boundary conditions

$$c_i \mid_{\lambda = 1} = c_{L,i} \tag{15}$$

and

$$\left. \frac{\partial c_i}{\partial \lambda} \right|_{\lambda = 0} = 0 \tag{16}$$

where λ stands for the dimensionless position inside the catalyst particle ($0 < \lambda < 1$). The intrinsic formation rate of component i, r_i, was calculated for each component from the rate equations (Eqs. 9 and 10), and the effective diffusion coefficient, $D_{\text{eff},i}$, was estimated with the equation

$$D_{\text{eff},i} = \frac{\epsilon_p}{\tau_p} D_i \tag{17}$$

The average values for aluminum oxide were used for the porosity (0.50) and tortuosity (4.0) of the pellet (Satterfield, 1970). Molecular diffusion coefficients (D_i) were calculated from the binary diffusion coefficients and liquid-phase molar fractions. Binary diffusion coefficients were estimated by the Wilke–Chang method (Reid et al., 1987).

Owing to the external heating and cooling, energy balances for bulk phases were not needed. Furthermore, the calculations showed that, under the conditions applied, the maximum temperature difference inside the catalyst particles was less than 0.3°C and, thus, the energy balance for the particle was omitted as well. Component balances inside a catalyst particle (Eq. 14) were discretized with respect to the position inside the particle by a 5-point central difference formula. The mass-transfer rates at the liquid–solid interface, $N_{LS,i}a_{LS}$, were then calculated for mole balance (Eq. 12) by summing up the average rates in each discretization piece. Thereafter, the linear system of ordinary differential equations (Eqs. 11 and 12) was integrated numerically by the backward-difference method.

Parameter Estimation and Results

Parameter estimation was done simultaneously with the integration of the reactor model equations. The objective function to be minimized was the sum of squares of the errors between the experimental and calculated molar fractions of the liquid product

$$Q = \sum_j \sum_i (x_{ij,\text{exp}} - x_{ij,\text{calc}})^2 \tag{18}$$

where j denotes analyzed product samples and i is the index for the components. The minimization of Eq. 18 was done with the Levenberg–Marquardt routine. All calculations were implemented in the in-house flow-sheet simulation and optimization programs FLOWBAT and KINFIT (Aittamaa and Keskinen, 2000), which include a data bank for thermodynamic properties, as well as VLE calculation routines and mathematical solvers. The correlation between the model parameters was reduced by writing the rate constants in Eqs. 9 and 10 in relative form

$$k = k_{\text{ref}} \exp\left[-\frac{E_{\text{app}}}{R}\left(\frac{1}{T} - \frac{1}{T_{\text{ref}}}\right)\right] \tag{19}$$

where 65°C was chosen as the reference temperature, T_{ref}. Thus, the estimated parameters were rate constants at the reference temperature, apparent activation energies, and adsorption equilibrium constants.

Table 2. Estimated Model Parameters for the Hydrogenation of TMP-1 and TMP-2 with 95% Confidence Intervals

Parameter	Estimated Value
$k_{\text{ref,TMP-1}} \dfrac{\text{mol}}{g_{Ni}h} \times \left(\dfrac{\text{m}^3}{\text{mol}}\right)^{3/2}$	$3.1 \pm 0.1 \times 10^{-3}$
$k_{\text{ref,TMP-2}} \dfrac{\text{mol}}{g_{Ni}h} \times \left(\dfrac{\text{m}^3}{\text{mol}}\right)^{3/2}$	$1.3 \pm 0.2 \times 10^{-3}$
$E_{\text{app,TMP-1}}$/kJ/mol	34 ± 2
$E_{\text{app,TMP-2}}$/kJ/mol	49 ± 6
$K_{\text{TMP-1}}$/m^3/mol	$6.0 \pm 0.5 \times 10^{-4}$
$K_{\text{TMP-2}}$/m^3/mol	$1.8 \pm 0.3 \times 10^{-4}$
K_{H}/m^3/mol	$0.16 \pm 0.03 \times 10^{-4}$
RSS	7.9×10^{-3}
RRMS	1.9×10^{-3}

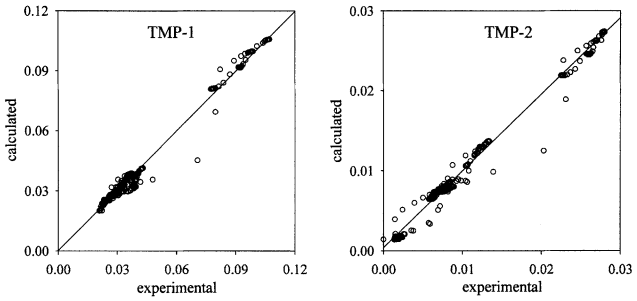

Figure 4. Experimental vs. calculated molar fractions of the reactants in the hydrogenation of TMP − 1 and TMP − 2.

The estimated model parameters and the 95% confidence limits are collected in Table 2. In addition, values of the residual sum of squares (RRS) of the 566 data points and the residual root mean square (RRMS) are presented. The estimated parameter values confirm the qualitative observation that TMP-1 is more reactive than TMP-2. At the reference temperature 65°C, the rate constant of TMP-1 is more than twice the corresponding value of TMP-2, and despite the stronger temperature dependency (higher E_{app}) of TMP-2, TMP-1 is the more reactive isomer throughout the temperature interval studied. The higher activation energy of TMP-2 also indicates that the energy barrier in the first hydrogen insertion is higher for TMP-2. This is probably due to steric factors: the double bond in TMP-1 is at the end of the carbon chain and more easily accessible for hydrogen. The adsorption equilibrium constant of hydrogen is an order of magnitude smaller than the corresponding constants of the alkenes. This result is consistent with the assumption that the catalyst deactivation was due to the formation of hydrogen-deficient species.

Figure 4 presents the experimental vs. calculated molar fractions of TMP-1 and TMP-2 of all data points. As can be seen from the figure, the model accurately describes the ex-

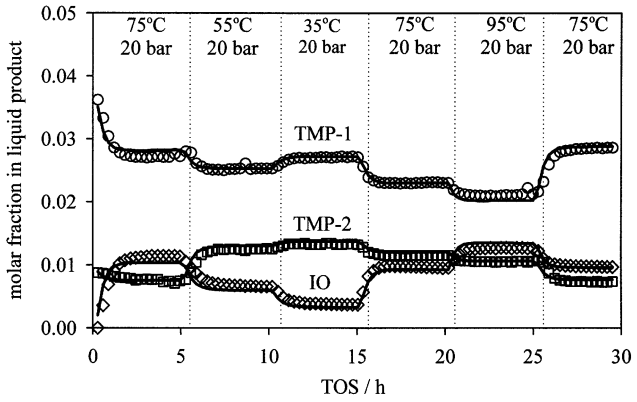

Figure 5. Experimental and calculated molar fractions of TMP-1, TMP-2, and isooctane in experiment B, where the total molar fraction of isooctenes was 5 mol %.

The feed was an equilibrium mixture of TMP-1 and TMP-2 during the first and last stage, and during the other stages the molar fraction of TMP-1 was 0.673. Temperature and pressure in each stage are shown at the top of the figure.

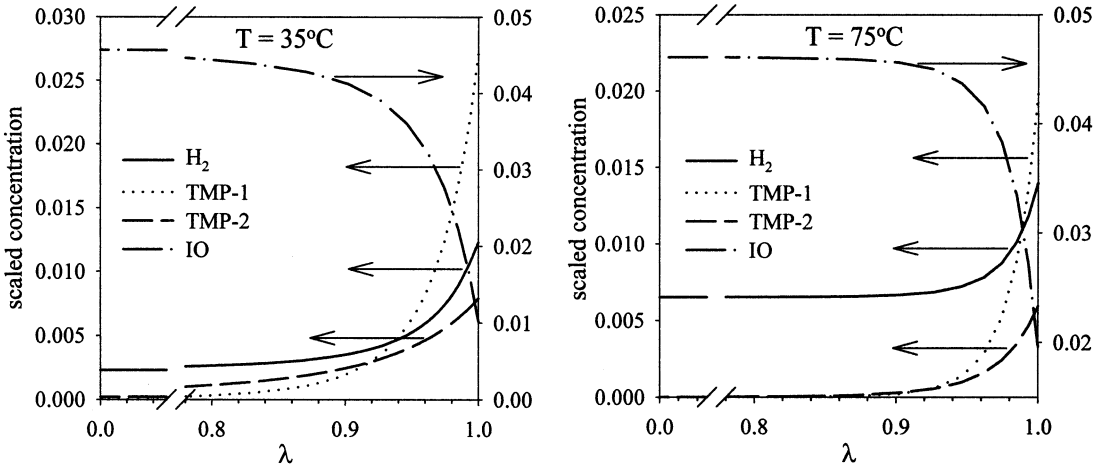

Figure 6. Concentration profiles of components inside catalyst particles at 35°C and 75°C under 20-bar hydrogen pressure.

The feed was an equilibrium mixture of TMP-1 and TMP-2 (4:1), and the initial mole fraction of isooctenes was 5 mol %.

perimental data under all reaction conditions tested. There is a little more scattering in the data of TMP-2 because, on average, the concentrations of TMP-2 in the feed were lower than the concentrations of TMP-1.

Figure 5 presents an example of the fit in a typical experimental run. The shapes of the dynamic model curves follow the experimental data points closely, both in the steady state and in the transient phases, indicating that the model for the reactor dynamics also is accurate. The feed in the figure is an equilibrium mixture of TMP-1 and TMP-2 (4:1) during the first and last stages (standard periods), and during the other stages the molar fraction of TMP-1 is 0.673. The total molar fraction of isooctenes is 5 mol % throughout the run.

Hydrogenation of both TMP-1 and TMP-2 was severely diffusion limited inside the catalyst pellets, even though the particle size used in the experiments was small (0.5–0.6 mm). The effectiveness factor for the formation of isooctane decreased from about 0.36 to 0.09 as the reaction temperature and pressure were increased and alkene content in the feed was decreased. Figure 6 shows concentration profiles of the components inside the catalyst particles at two different temperatures. As can be seen, concentrations of the limiting components are almost zero in the center of the pellet even at the lower temperature (35°C), and the profiles are still steeper at the higher temperature (75°C). Alkenes are the limiting components at both temperatures, although their total bulk concentration is higher than that of hydrogen. This is explained by the larger diffusion coefficient of hydrogen than of the alkenes.

Concluding Remarks

Hydrogenation of TMP-1 and TMP-2 to isooctane was studied in a three-phase reactor at 35 to 95°C and under hydrogen pressures from 10 bar to 40 bar. Kinetic experiments showed that Al_2O_3 supported nickel is a highly active and selective catalyst for these reactions. In addition to hydrogenation, some isomerization between TMP-1 and TMP-2 occurred. However, in all experiments the isomerization was slow compared to the hydrogenation. The effect of the catalyst deactivation, which was assumed to be due to the formation of hydrogen deficient species, was described with an empirical power-law model.

A kinetic model was proposed on the basis of the Horiuti–Polanyi mechanism, assuming that the formation of the half-hydrogenated intermediate is rate limiting. Kinetic parameters were estimated from the experimental data by nonlinear regression. Comparison of the experimental and calculated molar fractions in the product mixtures showed the model to predict the kinetic behavior of the system accurately.

Acknowledgments

The National Technology Agency of Finland (TEKES) and Fortum Oil and Gas Oy provided financial support. Mr. Petri Uusi-Kyyny (Laboratory of Chemical Engineering) is thanked for the distillation of the isooctene mixtures and Mr. Antti Hasanen for his help in obtaining the kinetic data.

Notation

a_{GL} = gas–liquid mass-transfer area/reactor volume
A = frequency factor of the rate constant
c_i = concentration of component i
D_i = molecular diffusion coefficient of component i
$D_{\text{eff},i}$ = effective diffusion coefficient of component i
E_{app} = apparent activation energy
F_i = molar flow rate of component i
G = gas phase
k = rate constant
K_i = adsorption equilibrium constant of component i
K_p = constant in Eq. 11 [$= 10^9$ mol/(m$^6\cdot$s)]
L = liquid phase
m_{cat} = mass of the catalyst
n_i = amount of i (mol) in the reactor
$N_{GL,i}$ = flux of component i at the gas–liquid interface
$N_{LS,i}$ = flux of component i at the liquid–solid interface
Q = objective function in Eq. 18
r_i = intrinsic reaction rate of i
R = gas constant [$= 8.3144$ J/(mol$\cdot$K)]
t = reaction time
T = temperature
V_R = reactor volume
x_i = molar fraction of component i in the liquid phase
Y = reaction intermediate

Greek letters

ϵ_p = porosity of the catalyst particle
κ_i = mass-transfer coefficient of component i
λ = dimensionless position inside the catalyst particle
Θ_i = fraction of the surface sites of component i on catalyst
ρ_p = bulk density of the catalyst particle

Literature Cited

Aittamaa, J., and K. Keskinen, *FLOWBAT—User's Instruction Manual*, Laboratory of Chemical Engineering, Helsinki University of Technology, Helsinki, Finland (2000).

Cortright, R. D., P. E. Levin, and J. A. Dumesic, "Kinetic Studies of Isobutane Dehydrogenation and Isobutene Hydrogenation Over Pt/Sn-Based Catalysts," *Ind. Eng. Chem. Res.*, **37**, 1717 (1998).

Fukushima, T., and A. Ozaki, "The Nature of Adsorbed Olefin Over Nickel Oxide as Revealed by Competitive Hydrogenation," *J. Catal.*, **59**, 465 (1979).

Horiuti, J., and M. Polanyi, "Exchange Reactions of Hydrogen on Metallic Catalysts," *Trans. Faraday Soc.*, **30**, 1164 (1934).

Jonker, G. H., J.-W. Veldsink, and A. A. C. M. Beenackers, "Intrinsic Kinetics of 9-Monoenic Fatty Acid Methyl Ester Hydrogenation over Nickel-Based Catalysts," *Ind. Eng. Chem. Res.*, **36**, 1567 (1997).

Karinen, R. S., M. S. Lylykangas, and A. O. I. Krause, "Reaction Equilibrium in the Isomerisation of 2,4,4-Trimethyl Pentenes," *Ind. Eng. Chem. Res.*, **40**, 1011 (2000).

Kiperman, S. L., "Some Problems of Chemical Kinetics in Heterogeneous Hydrogenation Catalysis," *Stud. Surf. Sci. Catal.*, **27**, 1 (1986).

McLeod, A. S., and L. F. Gladden, L. F., "The Influence of the Random Sequential Adsorption of Binary Mixtures on the Kinetics of Hydrocarbon Hydrogenation Reactions," *J. Chem. Phys.*, **110**, 4000 (1999).

Mintsa-Eya, V., L. Hilaire, A. Choplin, R. Touroude, and F. G. Gault, "The Reaction of Deuterium with Olefins on Nickel Catalysts: Evidence for Adsorbed Vinylic Species," *J. Catal.*, **82**, 267 (1983).

Moysan, J. M., M. J. Huron, H. Paradowski, and J. Vidal, "Prediction of the Solubility of Hydrogen in Hydrocarbon Solvents through Cubic Equations of State," *Chem. Eng. Sci.*, **38**, 1085 (1983).

Neurock, M., and R. A. van Santen, "A First Principles Analysis of C-H Bond Formation in Ethylene Hydrogenation," *J. Phys. Chem. B*, **104**, 11127 (2000).

Park, J., R. L. Robinson, and K. A. M. Gasem, "Solubilities of Hydrogen in Heavy Normal Paraffins at Temperatures from 323.2 to 423.2 K and Pressures to 17.4 MPa," *J. Chem. Eng. Data*, **40**, 241 (1995).

Peque, M., and R. Maurel, "Hydrogénation Catalytique: IV. Hydrogénation en Phase Liquide de Couples d'Oléfines Isomères de Position," *Bull. Soc. Chim. Fr.*, **6**, 1882 (1969).

Reid, R. C., J. M. Prausnitz, and B. E. Poling, *The Properties of Gases and Liquids*, McGraw-Hill, Boston (1987).

Sanfilippo, D., "Dehydrogenation of Paraffins—Key Technology for Petrochemicals and Fuels," *CATTECH*, **4**(1), 56 (2000).

Satterfield, C., *Mass Transfer in Heterogeneous Catalysis*, MIT Press, Cambridge, MA (1970).

Sloan, D., R. Birkhoff, M. F. Gilbert, M. Nurminen, and A. Pyhälahti, "Isooctane Production from C_4's as an Alternative to MTBE," *Proc. NPRA*, San Antonio, TX (2000).

Temkin, M. I., "The Kinetics of Some Industrial Heterogeneous Catalytic Reactions," *Adv. Catal.*, **28**, 173 (1979).

Trotta, R., M. Marchionna, and F. Amoretto, "An Iso-Octane Technology to Produce Alkylate Streams," *Today's Refinery*, **10**, 21 (1999).

Manuscript received July 10, 2002, and revision received Nov. 27, 2002.